

# PATIENT-SPECIFIC ARTERIAL FLOW SIMULATION WITH ADDITIONAL GEOMETRIC ELEMENTS

G. Tabor\*, D. Tame\*, F. Pierron<sup>†</sup>, P.G. Young\*, A. Watkinson<sup>‡</sup>, J. Thompson<sup>‡</sup>

\*School of Engineering, Computer Science and Mathematics  
University of Exeter, North Park Road, Exeter, EX4 7BB, UK  
e-mail: [g.r.tabor@ex.ac.uk](mailto:g.r.tabor@ex.ac.uk)

<sup>†</sup> Simpleware Ltd, Innovation Centre,  
Rennes Drive, Exeter, EX4 4RN

<sup>‡</sup> Royal Devon and Exeter Healthcare Trust

**Key words:** Computational Fluid Dynamics, Biomedical Simulation

**Abstract.** *Biomedical flow problems tend to involve domains which are geometrically complex over a range of scales. Much effort has gone into developing tools for generating computational meshes automatically from medical scan data (MRI, CT), allowing the easy creation of patient-specific models of the flow domain, and hence the investigation of flow under existing conditions. One obvious enhancement to this capability is to be able to interactively modify the geometry; this would for example allow the prior determination of the effect of certain surgical procedures. In this paper we report on the application of new techniques allowing the insertion of CAD models into the original scan data. The resulting computer program, ScanCAD, has been applied to three case studies illustrating the range of applications for such a technique.*

## 1 INTRODUCTION

Computational Fluid Dynamics (CFD) is proving to be a very valuable tool for understanding the mechanics of blood flow in the human circulatory system. A detailed understanding of the basic fluid dynamics is very valuable in the study of a range of circulatory conditions, such as wall deposition of plaque in stenosis and the flow through the resulting narrowed vessel. Experiment in such cases is difficult; in vivo studies are limited in scope, whilst in vitro reproduction of the exact conditions pertaining to a specific medical condition (for example an exact reproduction of a given geometry) is very challenging. In silico studies on the other hand, are able to provide a cornucopia of relevant data very cheaply, and in a way which is convenient for researchers to query to ascertain specific information.

### 1.1 Image-based mesh generation

One of the most serious challenges in applying CFD to biomedical flow problems is that of defining the geometry of the flow. Flows in arteries and other medically interesting flow

problems tend to involve geometries which are geometrically complex across a range of scales. Even finding a way to describe this complexity is quite challenging, and creating a mesh by hand to reflect the geometry is time consuming as well. To add to the complexity, such geometries are patient-specific, and the unique details of the geometry (often related to specific medical conditions) are of interest. Thus there has been a lot of interest in recent years in techniques for generating CFD meshes from medical scans such as MRI or CT scans. Such scanning techniques record 3d information (in the form of stacks of 2d images) of the interior of the patient, and thus can provide an exact record of the geometry of the patient. With an automated process for converting this to a FV or FE mesh, one can undertake patient-specific computations to look at the existing flow (pre- or post- medical intervention). The development of these computational tools is a major area of research in computational biofluid mechanics.

Such tools have been used to generate exact geometries for a number of studies, for instance the flow in significant sections of the arterial tree [5], and in single arteries [9]. Berthier et al [1] look at the influence of geometry on the blood flow, using 3 different reconstructions of a coronary vessel ranging from a simplistic constant-diameter tube to a geometrically accurate computational reconstruction. More localised investigations have also been carried out to look at the detailed flow, for example to investigate the wall shear stress – a significant issue in the development of atherosclerotic plaque deposition – in the vicinity of complex geometric structures such as the main bifurcation of the left coronary artery [8]. As they remark, this is data that could not be revealed from experimental methods, but is easily generated from CFD.

In general, we distinguish two types of approach to the problem of generating meshes from images : 'CAD'-type approaches and 'Voxel'-based approaches. In the former, the scan data is used to define the surface of the domain. This generates a 2d surface, parameterised in some way (usually as an STL file) which can be passed to an existing mesh generator such as Gambit, to create the mesh [10, 3]. Although this approach has some merit, as the complexity of the domain increases the problems of finding and handling the bounding surface increase considerably. The alternative, voxel-based methodology generates a volumetric mesh directly based on the pixelised scan data. In Exeter we have pioneered these techniques, implemented as a set of computer codes (ScanIP, ScanFE).

The process of generating a mesh involves first segmenting the different volumes of interest (VOI) from the 3D data. Both semi-automated and manual techniques are available within ScanIP, as well as a range of alternative image processing packages, to provide segmented masks. Techniques include noise filters, three dimensional thresholding tools through to bitmap painting. These VOI are then simultaneously meshed based on an orthotropic grid intersected by interfaces defining the boundaries. In effect a base Cartesian mesh of the whole volume defined by the sampling rate is tetrahedralised at boundary interfaces based on cutting planes defined by interpolation points. Smooth boundaries are obtained by adjusting the interpolation points in one, or a combination, of two ways: by setting points to reflect partial volumes or by applying a multiple material anti-aliasing

scheme. The process results in either a mixed tetrahedral/hexahedral mesh or a pure tetrahedral mesh and incorporates an adaptive meshing scheme. The approach is fully automated and robust creating smooth meshes with low element distortions regardless of the complexity of the segmented data.

## 1.2 Application of CFD to surgical procedures

CFD also finds application in investigating the effect of certain surgical procedures which may alter the structure of the artery or vein. This will typically involve inserting a man-made structure such as a stent into the body to enlarge or alter the geometry, or to bypass a blockage. Computational simulation has been used to investigate such structures, primarily in idealised situations (i.e. separate from the patient). Hyun et al [7, 6] have used idealised geometries to look at the effect of various surgical procedures on diseased carotid artery bifurcations, with considerable success. Meanwhile, de Hart et al [4] have investigated a design of stentless aortic valve using computational fluid-structure analysis under physiologically realistic operating conditions. Bypass grafts involve relieving a blockage by introducing a section of tube (synthetic or natural) to rejoin the two halves of the artery. This typically forms an end-to-side branch link. It seems likely that hemodynamic parameters such as wall shear stress and stress gradients are linked to long term failure of these grafts. Longest and Kleinstreuer [11] performed computational simulations of such structures using meshes generated using a physical reconstruction technique. This is a popular (and important) geometry to investigate, with several groups looking at the flow using similar in vitro/in silico models [12, 13]. However most procedures have to be carried out experimentally, such as the work of Rolland et al [15] investigating stent design by implanting into pigs.

## 1.3 Surgical and predictive modelling

The objective of our work is to combine the above; to allow the introduction of additional geometrical elements representing stents, bypasses etc. into the patient-specific computational model derived from the medical scan data. This could be achieved in a number of ways. The computational mesh created from the scan could be altered by the introduction or modification of cells within the mesh. This would entail creating some kind of ‘mesh modifier’ which would probably be too low level to be easily utilised. At a higher level of object manipulation, CAD-based image-to-mesh tools could be applied here by combining the STL surface generated by the tool with STL surfaces representing the additional elements using some kind of solid modelling software, before passing the resulting composite object to the mesh generator to produce the final mesh. However, since we are using voxel-based image-to-mesh conversion techniques, we have adopted a different approach, in which the original medical scan itself can be altered by introducing CAD models of additional geometric elements, which are then voxelised to form an additional mask within the scan. This approach has led to the creation of a third piece of software,

called ScanCAD, which permits the manipulation of STL-based surfaces from CAD models within the domain defined by the medical scan. The segmented scan data from ScanIP can be loaded into this code, and an arbitrary number of CAD models introduced and manipulated (for position and orientation) before being voxelised on the underlying pixel structure defined by the imaging. The resulting collection of segmented masks can be reimported into ScanIP for further mask manipulation, before being exported to ScanFE to generate the computational mesh.

The result is a computational mesh for the whole problem including patient-specific items (the arteries) and additional elements (stents, cannulae etc) which can be used to compute the flow through the composite domain. This could be used to do ‘predictive’ modelling to predict the effect of the particular surgical procedure being investigated. Thus, a standard treatment for atherosclerosis is the insertion of a stent, a metal device intended to hold the arterial walls open. We can generate a CAD model of the stent, position this within the segmented scan as it would be located by surgery, and calculate a priori the effect that this will have on the blood flow. Other types of intervention, such as bypass surgery or grafting, can similarly be modelled using this technology, thus making it a genuine predictive tool.

In this paper we present a number of small case studies on the flow through different structures; a simple bypass graft, an artery pierced with a cannula to inject a second stream of fluid, and a bypass used to relieve a stenosed internal carotid artery. The first two case studies are purely hypothetical examples, using real patient data (from MRI of a patient’s femoral artery) but introducing CAD models purely to reproduce generic surgical procedures. The final case study, on the stenosed ICA, uses genuine MRI data from a patient with this condition, for which followup scans of the patient after endarectomy surgery are available for comparison.

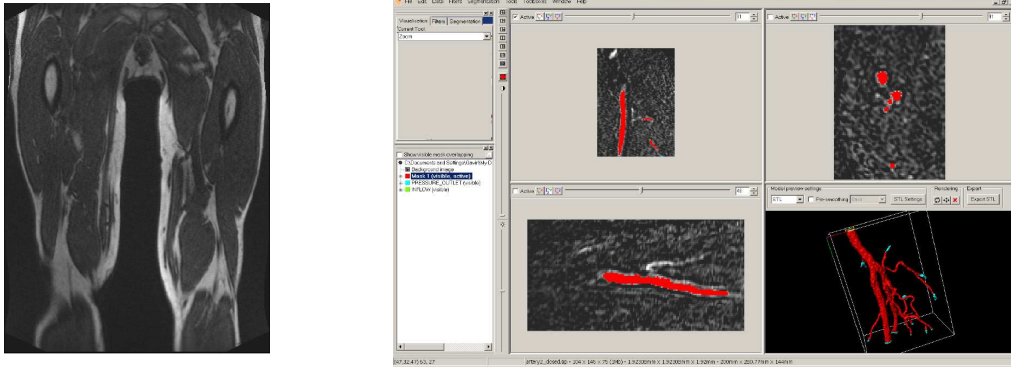


Figure 1: Left:Raw MRI slice of patient. Right: ScanIP segmentation to define artery network region.

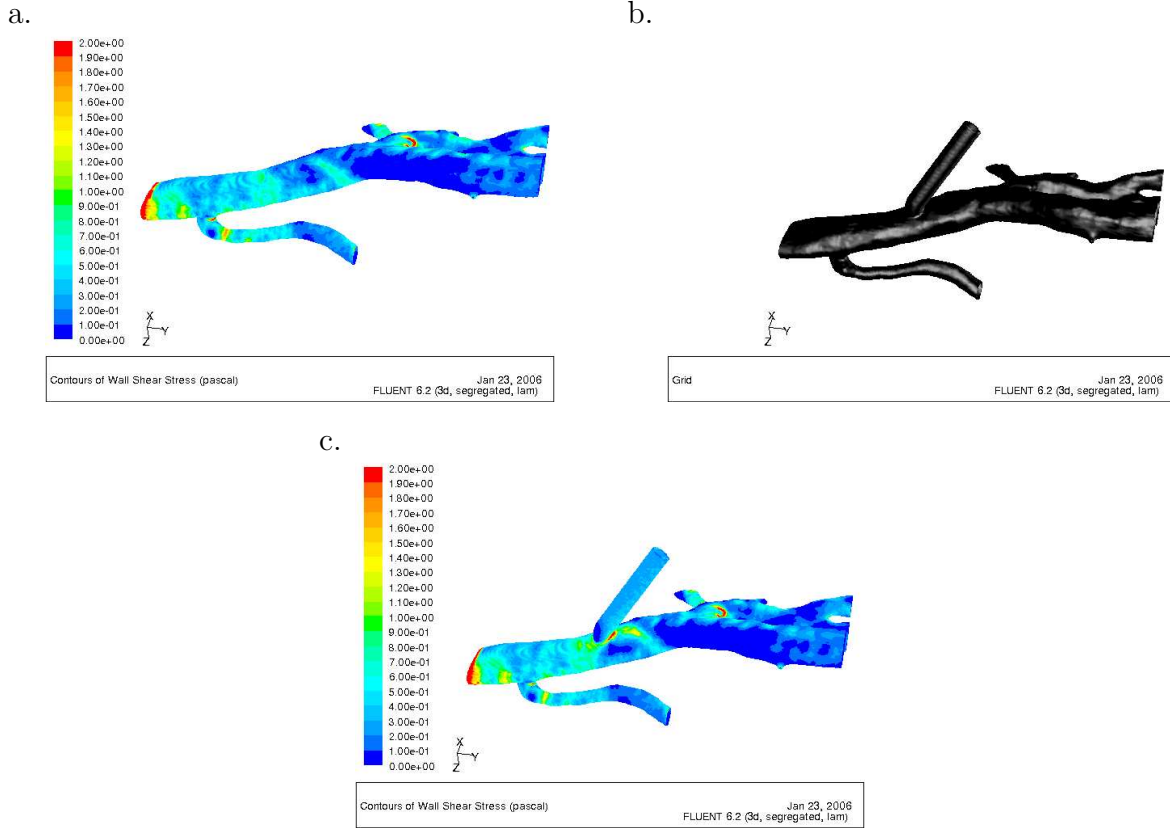


Figure 2: a. Basic section of femoral artery showing wall shear stress. b. Computational mesh for femoral artery with graft attached. c. Wall shear stress for femoral artery including attached graft.

## 2 CASE STUDY I: GRAFT

This case study, and the next, both rely on MRI data of an upper femoral artery taken in the RDEHT. This was chosen as a convenient dataset to experiment with the various geometrical changes made possible by ScanCAD, rather than representing any direct medical procedure. Figure 1 shows one of the individual MRI scans of the patient together with the ScanIP segmentation defining the arterial network of interest. Some preliminary numerical simulations were undertaken on this geometry, using a newtonian analog of blood (density  $\rho = 1000 \text{ kg/m}^3$ , relative viscosity 4) and a steady flow rate giving a Reynolds number of 500 (based on the hydraulic diameter of the inlet), representing conditions of laminar flow. The results in terms of wall shear stress (WSS) are shown in figure 2a. Next, a bypass graft was created using AutoCAD with a diameter of 4 mm and an angle of  $45^\circ$ ; this was introduced and positioned using ScanCAD, then combined with the original mask using ScanIP, before meshing using ScanFE. Figure 2b. shows the modified geometry, and figure 2c. the resulting WSS for the same inlet conditions. The introduced graft has resulted in a significant increase in WSS behind the point of

attachment.

### 3 CASE STUDY II: CANNULA

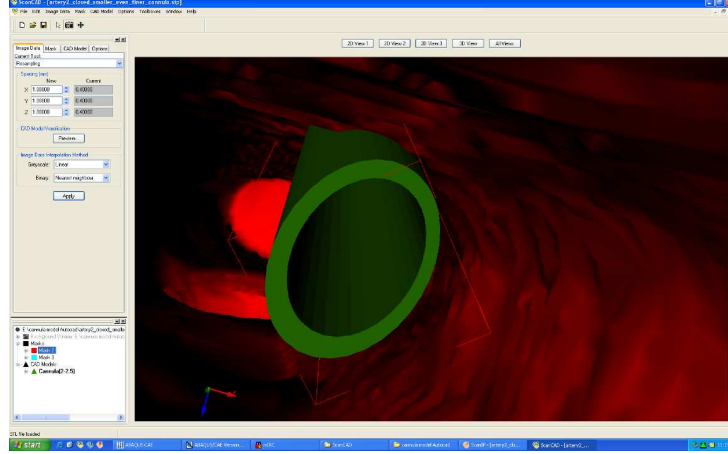


Figure 3: Screenshot of ScanCAD being used to position cannula into artery.

As a second demonstration of this technology an investigation has been carried out into the injection of fluid into the same artery through a cannula. Such a scenario is important in dialysis, where chemical mixing and altered flow patterns generated by the introduction of a second stream through a rigid cannula may have an effect on the development of stenosis close to the site of injection (c.f. [2]). The same arterial geometry was used for this case; but this time AutoCAD was used to construct a cannula in the form of a hollow cylinder of internal diameter 2 mm, outside diameter 2.5 mm truncated at 45° at one end. Figure 3 shows ScanCAD being used to position the cannula in the artery, prior to segmentation in ScanIP. After meshing by ScanFE the model was simulated in Fluent. The inlet conditions at the artery were the same as used in case I; as were the outlet conditions, whilst a flow speed of 20 cm/s was used at the cannula inlet. The same Newtonian blood analog was used as with case study I. Figures 4a-d. show the results from this steady-state calculation, with WSS (two views) on the artery walls, and velocities on a cutting plane (c., d.) revealing some of the interior structure of the flow. In the WSS plot, since the artery inlet velocity is uniform the WSS near the inlet is higher than it should be as the flow adapts; once it gets to the location of the cannula however, this effect has reduced and the effect of the presence of the cannula is visible both in the WSS and in the detail of the flow around and behind the cannula itself.

### 4 CASE STUDY III: CAROTID ARTERY

Data on atherosclerosis in the right internal carotid artery was obtained from a pre-operative scan on a single patient, taken at the Royal Devon and Exeter Hospital. This is

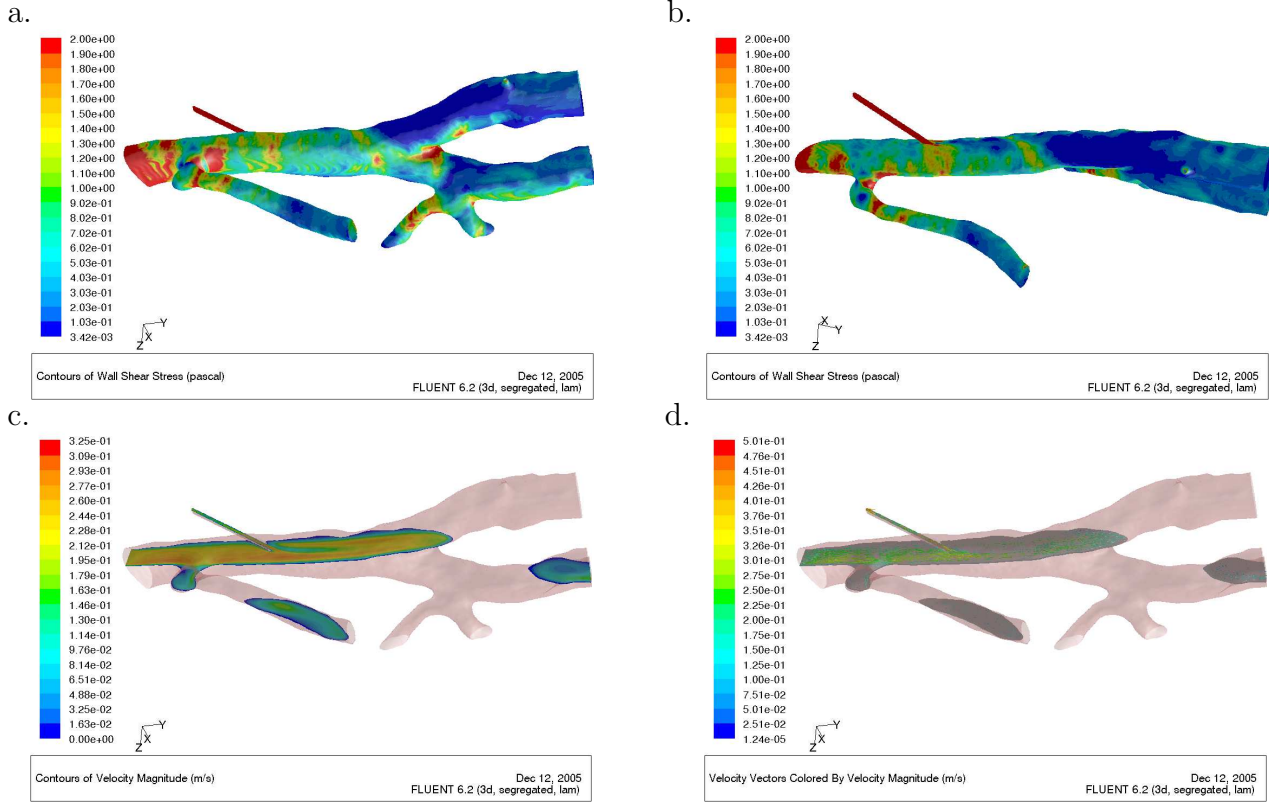


Figure 4: Various different visualisations of the artery pierced with a cannula. a.+b. wall shear stress for artery. c.contours of velocity magnitude on cutting plane through artery; d. velocity vectors on cutting plane through artery.

a serious medical condition; the internal carotid artery (ICA) on each side supplies blood to the brain via the Circle of Willis, and whilst stenosis on one side can be naturally compensated for by increased blood flow through the other side, plaque breaking off the stenosis will be carried into the brain, probably leading to a serious stroke. Some form of corrective surgery is usually applied in such cases. Pre- and post-operative scan data were available for this patient. ScanIP and ScanFE were used on the pre-operative data to segment out and mesh the whole arterial structure from the ascending aorta, comprising the left and right subclavian arteries and the left and right common carotid arteries, as shown in figure 5a. The common carotid arteries then divide into external carotid (ECA, supplying the face) and internal carotid (ICA, supplying the brain), which on the right side was severely blocked. We will refer to this as model IIIA, and it permitted a detailed examination of the preoperative flow towards the brain both through the stenosed right ICA, and through the healthy left side. The flow in these arteries of course merges again further up in the circle of Willis; one of the objectives of this piece of work was to examine the change in flow to the brain resulting from the surgical removal of the constriction.

With this in mind, a bypass structure (i.e. a tube of the correct dimensions) was created using SolidWorks and introduced into the scans using ScanCAD to mimic the effect of a possible surgical procedure. This is referred to as model IIIB. Finally, further MRI scans of the patient were taken after a conventional endarectomy operation had been performed to remove the plaque from the artery. Taking into account our experience with model IIIA, these scans were performed at a higher resolution in order to improve the model generated using ScanIP/ScanFE; this will be referred to as model IIIC.

All three models were run in Fluent, using approximate whole blood material properties [16] and a theoretical heart beat profile. This was a simple sinusoidal heartbeat cycle with a time period of 0.63 s and a blood pressure of 120/80 mmHg, giving an inlet velocity

$$U_{inlet} = \sqrt{\frac{214 \sin \omega t + 1069}{0.48\pi\rho}} \quad (1)$$

It was not possible to acquire the outlet pressures from the patient data in a usable form, so the outlet pressures were fixed based on the cross sectional area of the outlets relative to the total outlet area.

Results from the calculation were processed at the end time of the simulation, after a number of cardiac cycles had completed. Values of the instantaneous wall shear stress were particularly examined as this is believed to be an important parameter in determining issues such as plaque deposition. The data concerning the right ICA for model IIIA was unavailable; although the stenosis was clearly visible on the MRI scan, the resolution was too coarse and it proved impossible to segment it in ScanIP; in other words the artery was almost completely blocked. This resulted in increased flow up the right ECA and to a lesser extent up the left side of the system. In figure 6, high stresses are seen in the right ECA, again related to the closure of the right ICA. In case IIIB, the artificial bypass was inserted as close to the ends of the stenosis as possible; with an angle of 45° between the bypass and the core arterial geometry. This relieved the flow through the right ECA, although at the cost of creating a region of  $WSS < 0.5$  Pa, a factor which has been known to cause problems of intimal hyperplasia[14]. The data from these two models is easily comparable since they are based on the same initial scan. Model IIIC represented the situation after the actual surgical intervention, taken at a higher resolution, and of course at a later date. It shows very clearly the effect of the endarterectomy in increasing the size of the right ICA by approximately 3-4 times relative to its stenotic state, with corresponding changes in the flow state.

## 5 DISCUSSION AND CONCLUSIONS

The purpose of this paper has been to demonstrate a novel technology for including additional geometric elements into patient-specific models generated from medical scan data, rather than to perform any in-depth investigation into any of the flow conditions experienced in any of the case studies. That being so, it is possible to discuss how this



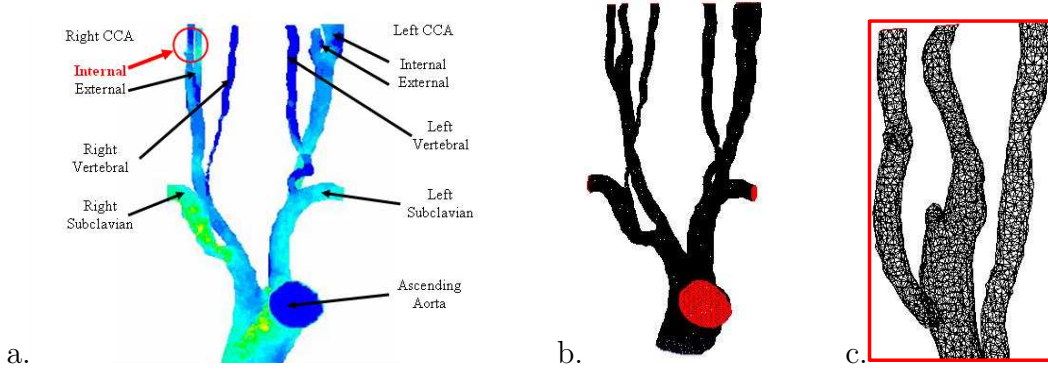


Figure 5: a. Segmented arterial structure ascending from the ascending aorta, showing position of the stenosis. b. Mesh generated by ScanFE. c. Closeup of mesh.

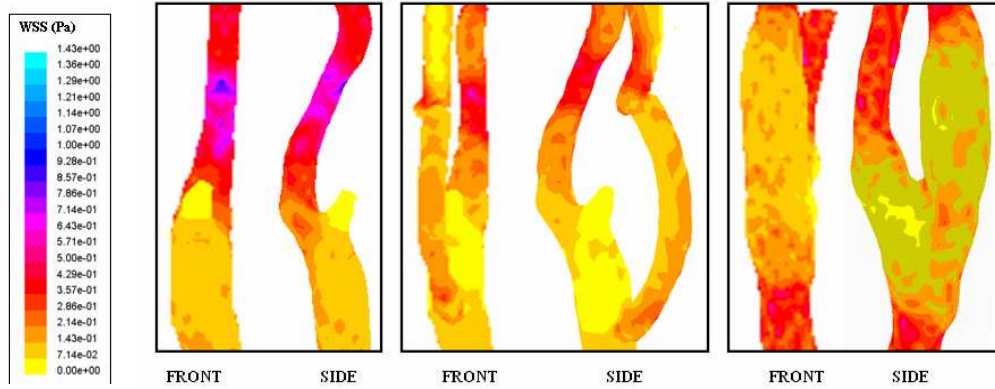


Figure 6: Wall shear stress for model IIIA (left) IIIB (centre) and IIIC (right).

‘editing’ ability may be used to undertake both investigative and predictive modelling of important surgical and medical procedures. The case studies themselves increase in complexity. Hence, case study I is of a relatively simple end-to-side arterial anastomosis. Various studies over the last three decades have established the importance of hemodynamic interactions with the arterial wall in provoking intimal hyperplasia and, ultimately, bypass graft failure. However, any quantitative study of these effects up until now has had to start with physically creating the geometry; either through surgery on a patient or the creation of some physical model. Hence, Longest and Kleinstreuer [11] undertake a lengthy model-building phase involving suturing PTFE tubing together, filling the resulting structure with polyurethane rubber and then digitising this internal cast using 3d laser scanning to generate the geometry for their computational model. Our techniques have allowed us to create an equivalent computational model on real, patient-specific data

in a much shorter timespan; typically a couple of hours to generate each specific model. This could allow a much wider exploration of the effect of different graft geometries on the flow and WSS. The second case study was geometrically more complex, and more challenging to set up as the cannula wall thickness 0.25 mm was comparable with the pixel resolution of the scan. However, again, we are able to create the individual models relatively quickly and easily, and this allows the exploration of a diversity of interesting cases.

Case study III is the most medically advanced of the three, being based on a real surgical case for which we have both pre- and post-surgical geometric information. This has allowed us to compare flows pre- and post-operatively based on the actual geometries. The surgical operation performed was basically the removal of the plaque from the artery rather than the insertion of any kind of stent or bypass; however we were also interested in exploring the use of the code for predictive modelling, and so investigated the effect of inserting a bypass into the arterial network. This sort of technique could potentially be used to explore the possible effects of surgery before it is implemented, in order to discern the best surgical approaches. Whilst it is unlikely that this would be done on a regular basis, it might be valuable to use this to undertake a survey of different surgical techniques as applied to particular classes of patient.

## 6 CONCLUSIONS

We have demonstrated the application of techniques for introducing additional geometric elements into CFD models derived from patient-specific MRI scans. The techniques are coded into a tool called ScanCAD, which can be used to interactively place CAD models into the segmented image stack from the MRI scan; this altered stack can then be converted into a finite volume mesh using our existing tools. The result is a powerful tool that can be used for both exploratory and predictive modelling; we have illustrated this with some results from three different case studies illustrating the potential for this technique.

Some of the work on this paper was undertaken with support from the Nuffield Foundation, grant number URB/33345.

## REFERENCES

- [1] B. Berthier, R. Bouzerar, and C. Legallais. Blood flow patterns in an anatomically realistic coronary vessel: influence of three different reconstruction methods. *Journal of Biomechanics*, 35:1347 – 1356, 2002.
- [2] A. Borg and L. Fuchs. Lif study of mixing in a model of a vein punctured by a cannula. *Int.J.Heat and Fluid Flow*, 23:664 – 670, 2002.
- [3] J. R. Cebal and R. Löhner. From medical images to anatomically accurate finite element grids. *Int.J.Num.Methods Eng.*, 51:985 – 1008, 2001.

- [4] J. de Hart, F.P.T. Baaijens, G.W.M. Peters, and P.J.G. Schreurs. A computational fluid-structure interaction analysis of a fiber-reinforced stentless aortic valve. *Journal of Biomechanics*, 36:699 – 712, 2003.
- [5] B. Ene-Iordache, G. Remuzzi, and A. Remuzzi. Computational fluid dynamics of a vascular access case for hemodialysis. *Journal of Biomechanical Engineering*, 123:284 – 292, 2001.
- [6] S. Hyun, C. Kleinstreuer, and J. P. Archie. Computational analysis of the effect of external carotid artery flow and occlusion on adverse carotid bifurcation hemodynamics. *J.Vasc.Surg*, 37:1248 – 1254, 2003.
- [7] S. Hyun, C. Kleinstreuer, P. W. Longest, and C. Chen. Particle-hemodynamics simulations and design options for surgical reconstruction of diseased carotid artery bifurcations. *J.Biomech.Engng*, 126(2):188 – 195, 2004.
- [8] S. Jin, Y Yang, J. Oshinski, A Tannenbaum, J. Gruden, and D Giddens. Flow patterns and wall shear stress distributions at atherosclerotic-prone sites in a human left coronary artery – an exploration using combined methods of ct and computational fluid dynamics. In *Proceedings of the 26th Annual International Conference of the IEEE EMBS, San Francisco, CA.*, pages 3789 – 3791, 2004.
- [9] B.M. Johnston, P. R. Johnston, S. Corney, and D. Kilpatrick. Non-newtonian blood flow in human right coronary arteries: steady-state simulations. *Journal of Biomechanics*, 37:709 – 720, 2004.
- [10] H. M. Ladak, J. S. Milner, and D. A. Steinman. Rapid three-dimensional segmentation of the carotid bifurcation from serial mr images. *J. Biomech. Eng.*, 122(1):96 – 99, February 2000.
- [11] P. W. Longest and C. Kleinstreuer. Numerical simulation of wall shear stress conditions and platelet localization in realistic end-to-side arterial anastomoses. *J.Biomech.Engng*, 125(5):671 – 681, 2003.
- [12] F. Loth, P. F. Fischer, N. Arslan, C. D. Bertram, S. E. Lee, T. J. Royston, W. E. Shaalan, and H. S. Bassiouny. Transitional flow at the venous anastomosis of an arteriovenous graft : Potential activation of the erk1/2 mechanotransduction pathway. *J.Biomech.Engng*, 125(1):49 – 61, 2003.
- [13] F. Loth, S. A. Jones, D. P. Giddens, H. S. Bassiouny, S. Glagov, and C.K. Zarins. Measurements of velocity and wall shear stress inside a ptfe vascular graft model under steady flow conditions. *J.Biomech.Engng*, 119:187 – 194, 1997.

- [14] S.L. Meyerson, C. L. Skelly, M. A. Curi, U.M. Shakur, J.E. Vosicky, S. Glagov, L.B. Schwartz abd T. Christen, and G. Gabbianni. The effects of extremely low shear stress on cellular proliferation and neointimal thickening in the failing bypass graft. *J.Vascular Surgery*, 34:90 – 97, 2001.
- [15] P. H. Roland, A-B. Charifi, C. Verrier, H. Bodard, A. Friggi, P. Piquet, G. Molin, and J-M. Bartolli. Hemodynamics and wall mechanics after stent placement in swine iliac arteries : Comparative results from six stent designs. *Radiology*, 213:229 – 246, 1999.
- [16] I. van Tricht, D. de Wachter, J. Tordoir, and P. Verdonck. Comparison of the hemodynamics in 6mm and 4-7mm hemodialysis grafts by means of cfd. *J.Biomech.*, 39:226 – 236, 2006.